Applications and Applied Mathematics: An International Journal (AAM)

Volume 16 | Issue 1 | Article 21

6-2021

Hybrid Algorithm for Singularly Perturbed Delay Parabolic Partial Differential Equations

Imiru T. Daba
Wollega University

Gemechis F. Duressa
Jimma University

Available at
http://pvamu.edu/aam
Appl. Appl. Math.
ISSN: 1932-9466

Applications and Applied Mathematics:
An International Journal
(AAM)

Vol. 16, Issue 1 (June 2021), pp. 397 – 416

Hybrid Algorithm for Singularly Perturbed Delay Parabolic Partial Differential Equations

[1*] Imiru Takele Daba and [2] Gemechis File Duressa

[1*] Department of Mathematics
Wollega University
Nekemte, Oromia, Ethiopia
imirutakele@gmail.com

[2] Department of Mathematics
Jimma University
Jimma, Oromia, Ethiopia
gammeef@gmail.com

*Corresponding Author

Received: October 18, 2020; Accepted: May 13, 2021

Abstract

This study aims at constructing a numerical scheme for solving singularly perturbed parabolic delay differential equations. Taylor's series expansion is applied to approximate the shift term. The obtained result is approximated by using the implicit Euler method in the temporal discretization on a uniform step size with the hybrid numerical scheme consisting of the midpoint upwind method in the outer layer region and the cubic spline method in the inner layer region on a piecewise uniform Shishkin mesh in the spatial discretization. The constructed scheme is an $\varepsilon-$uniformly convergent accuracy of order one. Some test examples are considered to testify the theoretical investigations.

Keywords: Singular perturbation problem; Delay parabolic differential equations; Implicit Euler method; Cubic spline method; Hybrid algorithm

MSC 2010 No.: 35K67, 65M06, 65M99

1. Introduction

A singularly perturbed delay differential equation (SPDDE) is a differential equation in which the highest order derivative is multiplied by a small parameter ε and containing a delay term. Such type of equation plays a prominent role in the mathematical modeling of various practical phenomena such as in modeling of neuronal variability (Stein (1967)), bistable devices (Derstine et al. (1982)), evolutionary biology (Wazewska et al. (1976)), variational problems of control theory (Glizer (2000)), to describe the human pupil-light reflex (Longtin and Milton (1988)), and many more.

Due to the existence of ε and a delay in the problem make the problem tiresome to be solved analytically. Hence, to solve this problem, one has to look for sounding numerical methods. Solving singularly perturbed delay differential equations using the classical methods on a uniform mesh, unable to provide an efficient numerical solution until we use $\Delta s \ll \varepsilon$, where Δs is the spatial step length. This drawback encourages researchers to develop the concept of robust numerical schemes for SPDDEs. In this context, the fitting techniques (i.e., operator and layer-adapted mesh) are a competitive computational scheme to overcome this drawback.

Various scholars have been developing $\varepsilon-$uniform numerical methods for singularly perturbed delay ordinary and partial differential equations with shift parameter(s) in the space variable and analyzing the effects of the shift parameters on the solution behavior. For instance, Adilaxmi et al. (2019) and Andargie and Reddy (2013) have developed $\varepsilon-$uniform numerical methods for singularly perturbed delay ODEs with small negative and positive shifts. Besides, the authors Ramesh and Kadalbajoo (2008), Kumar and Kadalbajoo (2011), Bansal et al. (2017), Kumar (2018), Rao and Chakravarthy (2019),Woldaregay and Duressa (2019), Daba and Duressa (2020), Ramesh and Priyanga (2019), Woldaregay and Duressa (2022b) and Woldaregay and Duressa (2022a) proposed different numerical methods based on fitting techniques for solving a second-order singularly perturbed delay parabolic partial differential equations (SPDPPDEs) with shift parameter(s) in the space variable and elucidated the influence of shift parameters on the boundary layer behavior of the solution.

However, numerical methods to solve SPDPPDE with delay in the spatial variable having an $\varepsilon-$uniform convergence for the past decades are still few and it needs a lot of investigations. The primary aim of this work is to construct an $\varepsilon-$uniform numerical scheme for solving SPDPPDEs with delay parameter in the space variable. The scheme is constructed based on the implicit Euler method for the temporal discretization on a uniform step size and hybrid algorithm based on the midpoint upwind method in the coarse mesh region and cubic spline difference method in the fine mesh region on a piecewise uniform Shishkin mesh for the spatial discretization. The efficiency of the scheme is shown by taking some test examples and comparing them with the numerical results we obtained by midpoint upwind, cubic spline method, and results in Kumar (2018) and Daba and Duressa (2020). The effect of the parameters on the boundary layer solutions are examined and presented in figures. The convergence of the constructed scheme is also investigated.

Throughout this manuscript, C represents a generic positive constant independent of the ε and mesh sizes.

2. Model Problem

In this paper, we consider the following problem on $D = \Omega \times \Gamma = (0,1) \times (0,T]$:

$$\begin{cases} \left(\frac{\partial}{\partial t} - \varepsilon^2 \frac{\partial^2}{\partial s^2} + \lambda(s)\frac{\partial}{\partial s}\right) v(s,t) + u(s)v(s-\delta,t) + \varrho(s)v(s,t) = \eta(s,t), (s,t) \in D, \\ v(s,0) = v_0(s), s \in \overline{\Omega}, \\ v(s,t) = \Upsilon_1(s,t), -\delta \leq s \leq 0, t \in \overline{\Gamma}, \\ v(1,t) = \Upsilon_2(1,t), t \in \overline{\Gamma}, \end{cases} \tag{1}$$

where $0 < \varepsilon \ll 1$ is a singular perturbation parameter and δ is a delay parameter of $o(\varepsilon)$. The functions $\lambda(s), u(s), \varrho(s), \eta(s,t), \Upsilon_1(s,t), \Upsilon_2(1,t)$ and $v_0(s)$ are considered to be sufficiently smooth, bounded and independent of ε. We also considered $u(s) + \varrho(s) \geq \zeta > 0, \;\; \forall s \in \overline{\Omega}$, for some positive constant ζ.

2.1. Properties of the continuous solution

When $\delta < \varepsilon$, the use of Taylor's series expansion for the terms containing shift arguments is valid (Tian (2002)). Consequently, we considered this case, and applying Taylor's series expansion, we obtain:

$$v(s-\delta,t) = v(s,t) - \delta\frac{\partial v(s,t)}{\partial s} + O(\delta^2). \tag{2}$$

Now inserting Equation (2) into Equation (1), we obtain

$$\begin{cases} L_\varepsilon v(s,t) = \eta(s,t), \\ v(s,0) = v_0(s), s \in \overline{\Omega}, \\ v(0,t) = \Upsilon_1(0,t), t \in \overline{\Gamma}, \\ v(1,t) = \Upsilon_2(1,t), t \in \overline{\Gamma}, \end{cases} \tag{3}$$

where $L_\varepsilon v(s,t) = \frac{\partial v(s,t)}{\partial t} - \varepsilon^2\frac{\partial^2 v(s,t)}{\partial s^2} + \theta(s)\frac{\partial v(s,t)}{\partial s} + \vartheta(s)v(s,t)$, $\theta(s) = \lambda(s) - \delta u(s)$ and $\vartheta(s) = u(s) + \varrho(s)$. Since $\theta(s) \geq \theta^* > 0$ and $\vartheta(s) \geq \vartheta^* > 0$ for some constants θ^* and ϑ^* the solution of Equation (3) exhibits boundary layer at $s = 1$ (Kumar (2018)). For small δ, Equation (1) and Equation (3) have almost equal approximate solution.

To elude conflict between boundary and initial condition, we suppose the compatibility conditions on the corner of the domain $(0,0)$ and $(0,1)$ as:

$$v_0(0) = \Upsilon_1(0,0), \quad v_0(1) = \Upsilon_2(1,0),$$

and

$$\begin{cases} \dfrac{\partial \Upsilon_1(0,0)}{\partial t} - \varepsilon^2 \dfrac{\partial^2 v_0(0)}{\partial s^2} + \theta(0)\dfrac{\partial v_0(0)}{\partial s} + \vartheta(0) v_0(0) = \eta(0,0), \\ \dfrac{\partial \Upsilon_2(1,0)}{\partial t} - \varepsilon^2 \dfrac{\partial^2 v_0(1)}{\partial s^2} + \theta(1)\dfrac{\partial v_0(1)}{\partial s} + \vartheta(1) v_0(1) = \eta(1,0). \end{cases}$$

Lemma 2.1. (Continuous Maximum Principle)

Let $\Xi(s,t) \in C^{2,1}(\overline{D})$. If $\Xi(s,t) \geq 0, \forall (s,t) \in \partial D$ ($\partial D = \overline{D} - D$) and $L_\varepsilon \Xi(s,t) \geq 0, \forall (s,t) \in D$, then $\Xi(s,t) \geq 0, \forall (s,t) \in \overline{D}$.

Proof:

Let $(s^*, t^*) \in \overline{D}$ be such that

$$\Xi(s^*, t^*) = \min_{(s,t) \in \overline{D}} \Xi(s,t),$$

and assume that $\Xi(s^*, t^*) < 0$, then $(s^*, t^*) \notin \partial D$. Also we have $\dfrac{\partial \Xi(s^*, t^*)}{\partial s} = 0$, $\dfrac{\partial \Xi(s^*, t^*)}{\partial t} = 0$, and $\dfrac{\partial^2 \Xi(s^*, t^*)}{\partial s^2} \geq 0$. Then

$$L_\varepsilon \Xi(s^*, t^*) = \frac{\partial \Xi(s^*, t^*)}{\partial t} - \varepsilon^2 \frac{\partial^2 \Xi(s^*, t^*)}{\partial s^2} + \theta(s^*) \frac{\partial \Xi(s^*, t^*)}{\partial s} + \vartheta(s^*) \Xi(s^*, t^*) < 0,$$

which contradicts the assumption made above. It follows that $\Xi(s^*, t^*) \geq 0$ and hence $\Xi(s,t) \geq 0, \forall (s,t) \in \overline{D}$. ■

Lemma 2.2. (Stability estimate)

The solution $v(s,t)$ of Equation (3) satisfies

$$\|v\| \leq (\vartheta^*)^{-1} \|\eta\| + \max\left\{|v_0(s)|, \max\left\{|\Upsilon_1(0,t)|, |\Upsilon_2(1,t)|\right\}\right\},$$

where $\|.\|$ is the L_∞ norm given by $\|v\| = \max_{(s,t) \in \overline{D}} |v(s,t)|$.

Proof:

Let $\Xi^{\pm}(s,t)$ be two barrier functions defined by:

$$\Xi^{\pm}(s,t) = (\vartheta^*)^{-1} \|\eta\| + \max\left\{|v_0(s)|, \max\left\{|\Upsilon_1(0,t)|, |\Upsilon_2(1,t)|\right\}\right\} \pm v(s,t).$$

Then at the initial value and the two end points, we have:

$$\begin{aligned} \Xi^{\pm}(s,0) &= (\vartheta^*)^{-1} \|\eta\| + \max\left\{|v_0(s)|, \max\left\{|\Upsilon_1(0,0)|, |\Upsilon_2(1,0)|\right\}\right\} \pm v(s,0) \geq 0, \\ \Xi^{\pm}(0,t) &= (\vartheta^*)^{-1} \|\eta\| + \max\left\{|v_0(0)|, \max\left\{|\Upsilon_1(0,t)|, |\Upsilon_2(1,t)|\right\}\right\} \pm v(0,t) \geq 0, \\ \Xi^{\pm}(1,t) &= (\vartheta^*)^{-1} \|\eta\| + \max\left\{|v_0(1)|, \max\left\{|\Upsilon_1(0,t)|, |\Upsilon_2(1,t)|\right\}\right\} \pm v(1,t) \geq 0, \end{aligned}$$

Using L_ε operator in Equation (3) on $\Xi^{\pm}(s,t)$ we have:

$$\begin{aligned} L_\varepsilon \Xi^{\pm}(s,t) &= \frac{\partial \Xi^{\pm}(s,t)}{\partial t} - \varepsilon^2 \frac{\partial^2 \Xi^{\pm}(s,t)}{\partial s^2} + \theta(s)\frac{\partial \Xi^{\pm}(s,t)}{\partial s} + \vartheta(s)\Xi^{\pm}(s,t), \\ &= \vartheta(s)\left((\vartheta^*)^{-1}\|\eta\|\right) + \vartheta(s)\left(\max\{|v_0(s)|, \max\{|\Upsilon_1(0,t)|, |\Upsilon_2(1,t)|\}\}\right) \pm L_\varepsilon v(s,t), \\ &\geq \vartheta(s)\left((\vartheta^*)^{-1}\|\eta\|\right) + \vartheta(s)\left(\max\{|v_0(s)|, \max\{|\Upsilon_1(0,t)|, |\Upsilon_2(1,t)|\}\}\right) \pm \eta(s,t), \\ &\geq \vartheta(s)\left(\max\{|v_0(s)|, \max\{|\Upsilon_1(0,t)|, |\Upsilon_2(1,t)|\}\}\right) + \vartheta(s)\,(\vartheta^*)^{-1}\|\eta\| \pm \eta(s,t). \end{aligned}$$

Using the fact $\vartheta(s) \geq \vartheta^* > 0$, we have $\vartheta(s)\,(\vartheta^*)^{-1} \geq 1$ and substituting it in the above inequality, we obtain:

$$L_\varepsilon \Xi^{\pm}(s,t) \geq 0, \quad \forall (s,t) \in \overline{D}, \text{ since } \|\eta\| \geq \eta(s,t).$$

Hence, by Lemma 2.1, we have $\Xi^{\pm}(s,t) \geq 0,\ \forall (s,t) \in \overline{D}$, which gives:

$$\|v\| \leq (\vartheta^*)^{-1}\|\eta\| + \max\{|v_0(s)|, \max\{|\Upsilon_1(0,t)|, |\Upsilon_2(1,t)|\}\}. \qquad \blacksquare$$

3. Description of the Numerical Scheme

3.1. Temporal Discretization

Consider the uniform time grid:

$$D_{\Delta t}^{M} = \left\{(s,t_j) : s \in \Omega, t_j = j\frac{T}{M} = j\Delta t,\ \ j = 0,1,2,\cdots,M\right\}.$$

Applying the implicit Euler scheme on t yields:

$$\begin{cases} \left(I + \Delta t L_\varepsilon^M\right)V^{j+1}(s) = \Delta t \eta^{j+1}(s) + V^j(s), \\ V(s,0) = V_0(s), s \in \overline{\Omega}, \\ V^{j+1}(0) = \Upsilon_1^{j+1}(0), j = 0,1,2,\cdots,M-1, \\ V^{j+1}(1) = \Upsilon_2^{j+1}(1), j = 0,1,2,\cdots,M-1, \end{cases} \tag{4}$$

where

$$L_\varepsilon^M V^{j+1}(s) = -\varepsilon^2 \frac{d^2 V^{j+1}(s)}{ds^2} + \theta(s)\frac{dV^{j+1}(s)}{ds} + \vartheta(s)V^{j+1}(s).$$

Lemma 3.1. (Semi-discrete Maximum Principle)

Let $\Xi^{j+1}(s) \in C^2(\overline{\Omega})$. If $\Xi^{j+1}(0) \geq 0$,, $\Xi^{j+1}(1) \geq 0$, and $\left(I + \Delta t L_\varepsilon^M\right)\Xi^{j+1}(s) \geq 0, \forall s \in \Omega$, then $\Xi^{j+1}(s) \geq 0, \forall s \in \overline{\Omega}$.

Proof:

Let $(s^*, t_{j+1}) \in \left\{(s,t_{j+1}) : s \in \overline{\Omega}\right\}$ be such that

$$\Xi^{j+1}(s^*) = \min_{s\in\overline{\Omega}} \Xi^{j+1}(s),$$

and suppose that $\Xi^{j+1}(s^*) < 0$, then we have $(s^*, t_{j+1}) \notin \{(0, t_{j+1}), (1, t_{j+1})\}$. Also we have $\dfrac{d\Xi^{j+1}(s^*)}{ds} = 0$, and $\dfrac{d^2\Xi^{j+1}(s^*)}{ds^2} \geq 0$. Then

$$\left(I + \Delta t L_\varepsilon^M\right) \Xi^{j+1}(s^*) = -\varepsilon^2 \frac{d^2\Xi^{j+1}(s^*)}{ds^2} + \theta(s^*) \frac{d\Xi^{j+1}(s^*)}{ds} + \vartheta(s^*)\Xi^{j+1}(s^*) < 0,$$

which contradicts our assumption $\left(I + \Delta t L_\varepsilon^M\right) \Xi^{j+1}(s) \geq 0, \forall s \in \Omega$. It follows that $\Xi^{j+1}(s^*) \geq 0$ and hence $\Xi^{j+1}(s) \geq 0, \forall s \in \overline{\Omega}$. ■

The differential operator $\left(I + \Delta t L_\varepsilon^M\right)$ satisfies a maximum principle and consequently, we obtain:

$$\left\| \left(I + \Delta t L_\varepsilon^M\right)^{-1} \right\| \leq \frac{1}{1 + \vartheta^* \Delta t}. \tag{5}$$

Lemma 3.2. (Local Error Estimate (LEE))

Suppose $\left|\dfrac{\partial^k v(s,t)}{\partial t^k}\right| \leq C,\ \forall\, (s,t) \in \overline{D}, k = 0, 1, 2$, then the LEE $e_{j+1} = v(s, t_{j+1}) - V^{j+1}(s)$ in the temporal direction of Equation (4) at $(j+1)\,th$ time level satisfies

$$\|e_{j+1}\| \leq C\,(\Delta t)^2\,.$$

Proof:

Since the function $V^{j+1}(s)$ satisfies

$$\left(I + \Delta t L_\varepsilon^M\right) V^{j+1}(s) - \Delta t \eta^{j+1}(s) = V^j(s), \tag{6}$$

and as the solution of Equation (1) is smooth enough, we have:

$$\begin{aligned} v(s, t_j) &= \left(I + \Delta t L_\varepsilon^M\right) v(s, t_{j+1}) - \Delta t \eta(s, t_{j+1}) + \int_{t_j}^{t_{j+1}} (t_j - \chi)\, \frac{\partial^2 v}{\partial t^2}\,(\chi)\, d\chi \\ &= \left(I + \Delta t L_\varepsilon^M\right) v(s, t_{j+1}) + O\left((\Delta t)^2\right). \end{aligned} \tag{7}$$

From Equation (6) and Equation (7), $e_{j+1} = v(s, t_{j+1}) - V^{j+1}(s)$ corresponding to Equation (4) satisfies

$$\begin{aligned} \left(I + \Delta t L_\varepsilon^M\right) e_{j+1} &= O\left((\Delta t)^2\right), \\ e_{j+1} &= \left(I + \Delta t L_\varepsilon^M\right)^{-1} O\left((\Delta t)^2\right), \\ e_{j+1}(0) &= e_{j+1}(1) = 0. \end{aligned} \tag{8}$$

Substituting Equation (5) in Equation (8), we obtain:

$$\|e_{j+1}\| \leq C\,(\Delta t)^2\,.$$ ■

Lemma 3.3. (Global error estimate (GEE))

The GEE E_j in the temporal direction of Equation (4) holds

$$\|E_j\|_\infty \leq C(\Delta t),\ \forall\, j \leq T/\Delta t.$$

Proof:

From Lemma 3.2, it follows that

$$\|E_j\|_\infty = \left\| \sum_{k=1}^{j} e_k \right\|_\infty \leq \|e_1\|_\infty + \|e_2\|_\infty + \cdots + \|e_j\|_\infty \leq C\left(\Delta t\right). \qquad \blacksquare$$

3.2. Spatial Discretization

Mesh Selection Strategy

Since the boundary value problem (4) exhibits a strong boundary layer at $s = 1$, we choose a piecewise-uniform Shishkin mesh and divide the domain $\overline{\Omega} = [0, 1]$ into two subintervals, namely $[0, 1 - \tau]$, and $1 - \tau, 1]$. Here the transition parameter τ is defined as:

$$\tau = \min\left(0.5, \tau_0 \varepsilon^2 \ln N\right), \qquad \tau_0 \geq \frac{1}{\theta^*}.$$

The mesh $\overline{\Omega}$ is given by:

$$s_i = \begin{cases} i\Delta s_i, & \text{for} \quad i = 0, 1, 2, \cdots, N/2, \\ 1 - \tau + (i - \dfrac{N}{2})\Delta s_i, & \text{for} \;\; i = N/2+1, N/2+2, \cdots, N, \end{cases}$$

where

$$\Delta s_i = s_i - s_{i-1} = \begin{cases} \dfrac{2(1-\tau)}{N}, & \text{for} \;\; i = 1, 2, 3, \cdots, N/2, \\ \dfrac{2\tau}{N}, & \text{for} \;\; i = N/2+1, N/2+2, \cdots, N. \end{cases}$$

3.2.1. *Hybrid Algorithm*

In this subsection, we approximate Equation (4) by using a hybrid algorithm that is based on the midpoint upwind method in the outside layer region (coarse mesh region) and cubic spline scheme in the inside layer region (fine mesh region).

Let us rewrite Equation (4) as:

$$\begin{cases} L_\varepsilon^M V^{j+1}(s) = \gamma^{j+1}(s), & s \in \overline{\Omega}, \;\; 0, 1, 2, \cdots, M-1, \\ V_0(s) = v_0(s), & s \in \overline{\Omega}, \\ V^{j+1}(0) = \Upsilon_1^{j+1}(0), & j = 0, 1, 2, \cdots, M-1, \\ V^{j+1}(1) = \Upsilon_2^{j+1}(1), & j = 0, 1, 2, \cdots, M-1, \end{cases} \tag{9}$$

where

$$L_\varepsilon^M V_i^{j+1} = -\varepsilon^2 \frac{d^2V^{j+1}(s)}{ds^2} + \theta(s)\frac{dV^{j+1}(s)}{ds} + Q(s)V^{j+1}(s),$$
$$Q(s) = \vartheta(s) + \frac{1}{\Delta t}, \qquad \gamma^{j+1}(s) = \eta^{j+1}(s) + \frac{V^j(s)}{\Delta t}.$$

Midpoint Upwind Method

The midpoint upwind method for Equation (9) takes the form:

$$L_{mu}^{N,M} V_i^{j+1} = \begin{cases} -\varepsilon^2 D_s^+ D_s^- V_i^{j+1} + \theta_{i-1/2} D_s^- V_i^{j+1} + Q_{i-1/2} V_{i-1/2}^{j+1} = \gamma_{i-1/2}^{j+1}, \\ V^{j+1}(0) = \Upsilon^{j+1}(0), \ \ j = 0,1,2,\cdots,M-1, \\ V^{j+1}(1) = \Upsilon^{j+1}(1), \ \ j = 0,1,2,\cdots,M-1, \end{cases} \tag{10}$$

where

$$D_s^- V_i^{j+1} = \frac{V_i^{j+1} - V_{i-1}^{j+1}}{\Delta s_i}, \ D_s^+ D_s^- V_{i,j+1} = \frac{2}{\Delta s_i + \Delta s_{i-1}} \left(\frac{V_{i+1}^{j+1} - V_i^{j+1}}{\Delta s_i} - \frac{V_i^{j+1} - V_{i-1}^{j+1}}{\Delta s_{i-1}} \right),$$
$$\theta_{i-1/2} = \left(\frac{\theta_i + \theta_{i-1}}{2} \right), Q_{i-1/2} = \left(\frac{Q_i + Q_{i-1}}{2} \right), \text{ and } \gamma_{i-1/2}^{j+1} = \left(\frac{\gamma_i^{j+1} + \gamma_{i-1}^{j+1}}{2} \right).$$

and $L_{mu}^{N,M} V_i^{j+1}$ is the midpoint upwind finite difference operator.

The resulting scheme gives the following system of equations:

$$L_{mu}^{N,M} V_i^{j+1} = s_i^- V_{i-1}^{j+1} + s_i^0 V_i^{j+1} + s_i^+ V_{i+1}^{j+1} = B_i^{j+1}, \qquad i = 1,2,3,\cdots,N-1, \qquad j = 0,1,2,\cdots,M-1, \tag{11}$$

where

$$s_i^- = \frac{-2\varepsilon^2}{\Delta s_{i-1}(\Delta s_i + \Delta s_{i-1})} - \frac{\theta_{i-1/2}}{\Delta s_i} + \frac{Q_{i-1/2}}{2},$$
$$s_i^0 = \frac{2\varepsilon^2}{\Delta s_i \Delta s_{i-1}} + \frac{\theta_{i-1/2}}{\Delta s_i} + \frac{Q_{i-1/2}}{2},$$
$$s_i^+ = \frac{-2\varepsilon^2}{\Delta s_i(\Delta s_i + \Delta s_{i-1})},$$
$$B_i^{j+1} = \gamma_{i-1/2}^{j+1}.$$

Cubic Spline Method

Now, we approximate the inside layer region of the resulting spatial equation (9) by applying the cubic spline method as described below. An interpolating cubic spline function $S^{j+1}(s)$ corresponding to the values $V^{j+1}(s_0), V^{j+1}(s_1), V^{j+1}(s_2), \cdots, V^{j+1}(s_N)$, of a function $V^{j+1}(s)$ at the points $s_0, s_1, s_2, \cdots, s_N$ and it satisfies the following properties:

(1) $S^{j+1}(s)$ coincides with a third-degree polynomial on each subinterval $[s_{i-1}, s_i], i = 1,2,3,\cdots,N$,

(2) $S^{j+1}(s) \in C^2(\overline{\Omega})$,
(3) $S^{j+1}(s_i) = V^{j+1}(s_i)$.

The cubic spline function $S^{j+1}(s)$ for $s \in [s_{i-1}, s_i]$, can be given as:

$$\begin{aligned} S^{j+1}(s) = \frac{(s_i - s)^3}{6\Delta s_i} M_{i-1} + \frac{(s - s_{i-1})^3}{6\Delta s_i} M_i + \left(V_{i-1}^{j+1} - \frac{h_i^2}{6} M_{i-1}\right)\left(\frac{s_i - s}{\Delta s_i}\right) \\ + \left(V_i^{j+1} - \frac{\Delta s_i^2}{6} M_i\right)\left(\frac{s - s_{i-1}}{\Delta s_i}\right), \end{aligned} \tag{12}$$

where $M_i = \dfrac{d^2 S^{j+1}(s_i)}{ds^2}, \;\; i = 1, 2, 3, \cdots, N.$

Following Priyadharshini (2010), we obtain:

$$\begin{aligned} &\frac{\Delta s_i}{6} M_{i-1} + \frac{\Delta s_i + \Delta s_{i+1}}{3} M_i + \frac{\Delta s_{i+1}}{6} M_{i+1} \\ &\qquad = \frac{V^{j+1}(s_{i+1}) - V^{j+1}(s_i)}{\Delta s_{i+1}} - \frac{V^{j+1}(s_i) - V^{j+1}(s_{i-1})}{\Delta s_i}, \\ &\qquad i = 1, 2, 3, \cdots, N-1, j = 1, 2, 3, \cdots, M-1 \end{aligned} \tag{13}$$

Using Taylor's series approximations for $V^{j+1}(s_k), k = i \pm 1$ in the spatial variable, we have:

$$V^{j+1}(s_{i-1}) \approx V^{j+1}(s_i) - \Delta s_{i-1} \frac{dV^{j+1}(s_i)}{ds} + \frac{\Delta s_{i-1}^2}{2} \frac{d^2 V^{j+1}(s_i)}{ds^2}, \tag{14}$$

$$V^{j+1}(s_{i+1}) \approx V^{j+1}(s_i) + \Delta s_i \frac{dV^{j+1}(s_i)}{ds} + \frac{\Delta s_i^2}{2} \frac{d^2 V^{j+1}(s_i)}{ds^2}. \tag{15}$$

Multiplying Equation (14) by $\Delta s_i^2 / \Delta s_{i-1}^2$ and then subtracting the resulting equations from Equation (15) , we have:

$$\frac{dV^{j+1}(s_i)}{ds} \approx \frac{\left(-\Delta s_i^2 V^{j+1}(s_{i-1}) + (\Delta s_i^2 - \Delta s_{i-1}^2) V^{j+1}(s_i) + \Delta s_{i-1}^2 V^{j+1}(s_{i+1})\right)}{\Delta s_i \Delta s_{i-1}(\Delta s_i + \Delta s_{i-1})}. \tag{16}$$

Similarly, multiplying Equation (14) by $\Delta s_i / \Delta s_{i-1}$ and then adding the resulting equations to Equation (15), we get:

$$\frac{d^2 V^{j+1}(s_i)}{ds^2} \approx \frac{(\Delta s_i^2 V^{j+1}(s_{i-1}) - (\Delta s_i + \Delta s_{i-1}) V^{j+1}(s_i) + \Delta s_{i-1} V^{j+1}(s_{i+1}))}{\Delta s_i \Delta s_{i-1}(\Delta s_i + \Delta s_{i-1})}. \tag{17}$$

Inserting Equation (16) and Equation (17) in $\dfrac{dV^{j+1}(s_{i+1})}{ds} \approx \dfrac{dV^{j+1}(s_i)}{ds} + \Delta s_i \dfrac{d^2 V^{j+1}(s_i)}{ds^2}$ and $\dfrac{dU^{j+1}(s_{i-1})}{ds} \approx \dfrac{dV^{j+1}(s_i)}{ds} - \Delta s_{i-1} \dfrac{d^2 V^{j+1}(s_i)}{ds^2}$, we obtain:

$$\frac{dV^{j+1}(s_{i-1})}{ds} \approx \frac{-\left(\Delta s_i^2 + 2\Delta s_i \Delta s_{i-1}\right) V^{j+1}(s_{i-1}) + (\Delta s_i + \Delta s_{i-1})^2 V^{j+1}(s_i) - \Delta s_{i-1}^2 V^{j+1}(s_{i+1})}{\Delta s_i \Delta s_{i-1}(\Delta s_i + \Delta s_{i-1})}, \tag{18}$$

$$\frac{dV^{j+1}(s_{i+1})}{ds} \approx \frac{\Delta s_i^2 V^{j+1}(s_{i-1}) - (\Delta s_i + \Delta s_{i-1})^2 V^{j+1}(s_i) + \left(\Delta s_i^2 + 2\Delta s_i \Delta s_{i-1}\right) V^{j+1}(s_{i+1})}{\Delta s_i \Delta s_{i-1}(\Delta s_i + \Delta s_{i-1})}. \tag{19}$$

Rearranging Equation (9) at $s = s_k, k = i, i \pm 1$ as:

$$\varepsilon^2 M_k = \theta_k \frac{dV^{j+1}(s_k)}{ds} + Q_k V^{j+1}(s_k) - \gamma^{j+1}(s_k). \tag{20}$$

Substituting Equations (16), (18), and (19) into Equation (20) and inserting the resulting equation into Equation (13) yields:

$$L_{cs}^{N,M} = r_i^- V_{i-1}^{j+1} + r_i^0 V_i^{j+1} + r_i^+ V_{i+1}^{j+1} = F_i^{j+1}, i = 1, 2, 3 \cdots, N-1, j = 0, 1, 2, \cdots, M-1, \tag{21}$$

where L_{cs}^N is the cubic spline operator,

$$r_i^- = \frac{\theta_{i-1}(\Delta s_i + 2\Delta s_{i-1})}{2(\Delta s_{i-1} + \Delta s_i)} + \frac{\Delta s_{i-1} Q_{i-1}}{2} - \frac{\Delta s_i \theta_i}{\Delta s_{i-1}} + \frac{\theta_{i+1}\Delta s_i^2}{2\Delta s_{i-1}(\Delta s_{1-1} + \Delta s_i)} - \frac{3\varepsilon^2}{\Delta s_{i-1}},$$

$$r_i^0 = \frac{\theta_{i-1}(\Delta s_{i-1} + \Delta s_i)}{2\Delta s_i} + \frac{\theta_i(\Delta s_i^2 - \Delta s_{i-1}^2)}{\Delta s_i \Delta s_{i-1}} + (\Delta s_i + \Delta s_{i-1})Q_i - \frac{\theta_{i+1}(\Delta s_{i-1} + \Delta s_i)}{2\Delta s_{i-1}} + \frac{3\varepsilon^2(\Delta s_i + \Delta s_{i-1})}{\Delta s_i \Delta s_{\Delta s_{i-1}}},$$

$$r_i^+ = -\frac{\theta_{i-1}\Delta s_{i-1}^2}{2\Delta s_i(\Delta s_{i-1} + \Delta s_i)} + \frac{\Delta s_i Q_{i+1}}{2} + \frac{\Delta s_{i-1}\theta_i}{\Delta s_i} + \frac{\theta_{i+1}(\Delta s_{i-1} + 2\Delta s_i)}{2(\Delta s_i + \Delta s_{i-1})} - \frac{3\varepsilon^2}{\Delta s_i},$$

$$F_i^{j+1} = \frac{\Delta s_{i-1}}{2}\gamma_{i-1}^{j+1} + (\Delta s_i + \Delta s_{i-1})\gamma_i^{j+1} + \frac{\Delta s_i}{2}\gamma_{i+1}^{j+1}.$$

The total discrete scheme takes the form:

$$L_{hyb}^{N,M} V_i^{j+1} = \begin{cases} L_{mu}^{N,M} V_i^{j+1} = \gamma_{i-1/2,j+1}, \quad i = 1, 2, 3, \cdots, N/2, \quad j = 0, 1, 2, \cdots, M-1, \\ L_{cs}^{N,M} V_i^{j+1} = \gamma_i^{j+1}, \quad i = N/2+1, N/2+2, \cdots, N, \quad j = 0, 1, 2, \cdots, M-1, \\ V_0^{j+1} = \Upsilon_1^{j+1}(0), \quad j = 0, 1, 2, \cdots, M-1, \\ V_N^{j+1} = \Upsilon_2^{j+1}(1), \quad j = 0, 1, 2, \cdots, M-1, \\ V_{i,0} = V(s_i, 0), \quad i = 0, 1, 2, \cdots, N. \end{cases} \tag{22}$$

Thus, we obtain the system of linear equations as:

$$R_i^- V_{i-1}^{j+1} + R_i^0 V_i^{j+1} + R_i^+ V_{i+1}^{j+1} = G_i^{j+1}, \quad i = 1, 2, 3, \cdots, N-1, j = 0, 1, 2, \cdots, M-1, \tag{23}$$

where

$$R_i^- = \begin{cases} \dfrac{-2\varepsilon^2}{\Delta s_{i-1}(\Delta s_i + \Delta s_{i-1})} - \dfrac{\theta_{i-1/2}}{\Delta s_i} + \dfrac{Q_{i-1/2}}{2}, \quad i = 1, 2, 3, \cdots, N/2, \\ \dfrac{\theta_{i-1}(\Delta s_i + 2\Delta s_{i-1})}{2(\Delta s_{i-1} + \Delta s_i)} + \dfrac{\Delta s_{i-1} Q_{i-1}}{2} - \dfrac{\Delta s_i \theta_i}{\Delta s_{i-1}} + \dfrac{\theta_{i+1}\Delta s_i^2}{2\Delta s_{i-1}(\Delta s_{1-1} + \Delta s_i)} - \dfrac{3\varepsilon^2}{\Delta s_{i-1}}, \\ \qquad i = N/2+1, N/2+2, \cdots, N-1, \end{cases}$$

$$R_i^0 = \begin{cases} \dfrac{2\varepsilon^2}{\Delta s_i \Delta s_{i-1}} + \dfrac{\theta_{i-1/2}}{\Delta s_i} + \dfrac{Q_{i-1/2}}{2}, \quad i = 1, 2, 3, \cdots, N/2, \\ \dfrac{\theta_{i-1}(\Delta s_{i-1} + \Delta s_i)}{2\Delta s_i} + \dfrac{\theta_i(\Delta s_i^2 - \Delta s_{i-1}^2)}{\Delta s_i \Delta s_{i-1}} + (\Delta s_i + \Delta s_{i-1})Q_i - \dfrac{\theta_{i+1}(\Delta s_{i-1} + \Delta s_i)}{2\Delta s_{i-1}} \\ \quad + \dfrac{3\varepsilon^2(\Delta s_i + \Delta s_{i-1})}{\Delta s_i \Delta s_{i-1}}, i = N/2+1, N/2+2, \cdots, N-1, \end{cases}$$

$$R_i^+ = \begin{cases} \dfrac{-2\varepsilon^2}{\Delta s_i(\Delta s_i + \Delta s_{i-1})}, \quad i = 1, 2, 3, \cdots, N/2, \\ -\dfrac{\theta_{i-1}\Delta s_{i-1}^2}{2\Delta s_i\left(\Delta s_{i-1} + \Delta s_i\right)} + \dfrac{\Delta s_i Q_{i+1}}{2} + \dfrac{\Delta s_{i-1}\theta_i}{\Delta s_i} + \dfrac{\theta_{i+1}(\Delta s_{i-1} + 2\Delta s_i)}{2(\Delta s_i + \Delta s_{i-1})} - \dfrac{3\varepsilon^2}{\Delta s_i}, \\ i = N/2+1, N/2+2, \cdots, N-1, \end{cases}$$

$$G_i^{j+1} = \begin{cases} B_i^{j+1}, \quad i = 0, 1, 2, \cdots, N/2, \ j = 0, 1, 2, \cdots, M-1, \\ F_i^{j+1}, \quad i = N/2+1, N/2+2, \cdots, N-1, \ j = 0, 1, 2, \cdots, M-1. \end{cases}$$

4. Error Analysis

To show the convergence of the scheme (22), we decompose the obtained solution into regular part Y_i^{j+1} and singular part Z_i^{j+1} as:

$$V_i^{j+1} = Y_i^{j+1} + Z_i^{j+1}, \tag{24}$$

where Y_i^{j+1} is

$$\begin{cases} L_{hyb}^{N,M} Y_i^{j+1} = \begin{cases} \gamma_i^{j+1}, \ i = \ 0, 1, 2, \cdots, N/2, \ \ j = 0, 1, 2, \cdots, M-1, \\ \gamma_{i-1/2}^{j+1}, \ N/2+1, N/2+2, \cdots, N, \ j = 0, 1, 2, \cdots, M-1, \end{cases} \\ Y_0^{j+1} = Y(0, t_{j+1}), \ \ j = 0, 1, 2, \cdots, M-1, \\ Y_1^{j+1} = Y(1, t_{j+1}), \quad j = 0, 1, 2, \cdots, M-1, \\ Y(i, 0) = Y(s_i, 0), \quad i = 0, 1, 2, \cdots, N, \end{cases}$$

and Z_i^{j+1} is

$$\begin{cases} L_{hyb}^{N,M} Z_i^{j+1} = 0, \ i = 0, 1, 2, \cdots, N, \ j = 0, 1, 2, \cdots, M-1, \\ Z_0^{j+1} = Z(0, t_{j+1}), \ \ j = 0, 1, 2, \cdots, M-1, \\ Z_1^{j+1} = Z(1, t_{j+1}), \ \ j = 0, 1, 2, \cdots, M-1, \\ Z(i, 0) = Z(s_i, 0), \ \ i = 0, 1, 2, \cdots, N. \end{cases}$$

Now, the error is

$$\left(v - V\right)\left(s_i, t_{j+1}\right) = \left(y - Y\right)\left(s_i, t_{j+1}\right) + \left(z - Z\right)\left(s_i, t_{j+1}\right).$$

Lemma 4.1.

The solution of the regular part satisfies

$$|(y - Y)(s_i, t_{j+1})| \le C\left(\Delta t + N^{-1}(\varepsilon^2 + N^{-1})\right).$$

Proof:

From the truncation error estimate (TEE), we have:

$$\left|L_{hyb}^{N,M}\left(y-Y\right)\left(s_i,t_{j+1}\right)\right| \leq C\left(\Delta t+\varepsilon^2\int_{s_{i-1}}^{s_{i+1}}\left|y^{'''}(\omega,t_{j+1})\right|d\omega+\Delta s_i\int_{s_{i-1}}^{s_{i+1}}\left|y^{'''}(\omega,t_{j+1})\right|d\omega\right)$$
$$\leq C\left(\Delta t+\left(\Delta s_{i+1}+\Delta s_i\right)\varepsilon^2+\Delta s_i^2\right).$$

Let $H=\max\left\{\Delta s_i\right\}$. Then, we have:

$$\left|L_{hyb}^{N,M}\left(y-Y\right)\left(s_i,t_{j+1}\right)\right| \leq C\left(\Delta t+H\left(\varepsilon^2+H\right)\right).$$

Let us consider the barrier functions for $i=1,2,3,\cdots,N-1, j\Delta t\leq T$ $\beta^{\pm}(s_i,t_{j+1}) = C\left(\Delta t+H\left(\varepsilon^2+H\right)\right)\pm(y-Y)(s_i,t_{j+1})$. Clearly, we have $\beta^{\pm}(s_0,t_{j+1})\geq 0$, $\beta^{\pm}(s_N,t_{j+1})\geq 0$ and $L_{hyb}^{N,M}\beta^{\pm}(s_i,t_{j+1})\geq 0$.

Thus, an application of discrete maximum principle gives:

$$|(y-Y)(s_i,t_{j+1})|\leq C\left(\Delta t+N^{-1}(\varepsilon^2+N^{-1})\right).$$ ■

Lemma 4.2.

The solution of the singular part satisfies

$$|(z-Z)(s_i,t_{j+1})|\leq C\left(\Delta t+N^{-2}(\ln N)^2\right).$$

Proof:

From the TEE, we have:

$$\left|L_{hyb}^{N,M}\left(z-Z\right)\left(s_i,t_{j+1}\right)\right|\leq\varepsilon^2\Delta s_i^2\left\|z^{(4)}(s_i,t_{j+1})\right\|\leq C\left(\Delta t+N^{-2}(\ln N)^2\right).$$

By considering the barrier functions for $i=1,2,\cdots,N-1, j\Delta t\leq T$,

$$\beta^{\pm}(s_i,t_{j+1})=C\left(\Delta t+N^{-2}(\ln N)^2\right)\pm\left|\left(z-Z\right)\left(s_i,t_{j+1}\right)\right|,$$

we obtain $\beta^{\pm}(s_0,t_{j+1})\geq 0$, $\beta^{\pm}(s_N,t_{j+1})\geq 0$ and $L_{hyb}^{N,M}\beta^{\pm}(s_i,t_{j+1})\geq 0$. Therefore, an application of discrete maximum principle gives:

$$\left|\left(z-Z\right)\left(s_i,t_{j+1}\right)\right|\leq C\left(\Delta t+N^{-2}(\ln N)^2\right).$$ ■

Lemma 4.3.

Let $v(s,t)$ be the solution of the problem (1) and $V(s,t)$ be the numerical solution of the corresponding discrete scheme (22). Then at each mesh point $(s_i,t_{j+1})\in\overline{D}$, then we have:

$$\left|\left(v-V\right)\left(s_i,t_{j+1}\right)\right|\leq C\left(\Delta t+N^{-2}(\ln N)^2\right).$$

Proof:

The proof follows from the triangular inequality and Lemmas 4.1 and 4.2. ■

5. Numerical Examples

As the exact solutions of the considered examples are not known, the maximum pointwise error for these examples are computed by using the double mesh principle as given in Doolan et al. (1980):

$$E_{\varepsilon,\delta}^{N,M} = \max_{1\le i,j\le N-1,M-1} \left| V_{i,j}^{N,M} - V_{i,j}^{2N,2M} \right|,$$

where $V_{i,j}^{N,M}$ and $V_{i,j}^{2N,2M}$ are the computed numerical solutions obtained on the mesh $D^{N,M} = \Omega^N \times \Gamma^M$ and $D^{2N,2M} = \Omega^{2N} \times \Gamma^{2M}$ respectively, N and M are mesh intervals in the spatial and temporal direction respectively.

For any value of N and M the $\varepsilon-$uniform errors $\left(E^{N,M}\right)$ and the $\varepsilon-$uniform order of convergence $\left(r^{N,M}\right)$ are calculated by the following formula,

$$E^{N,M} = \max_{\varepsilon,\delta} \left(E_{\varepsilon,\delta}^{N,M} \right), \text{ and } r^{N,M} = \log_2 \left(\frac{E^{N,M}}{E^{2N,2M}} \right),$$

respectively.

Example 5.1.

Consider the following SPPPDDE:

$$\begin{cases} \left(\dfrac{\partial}{\partial t} - \varepsilon^2 \dfrac{\partial^2}{\partial s^2} + (2+s+s^2)\dfrac{\partial}{\partial s} \right) v(s,t) + (\dfrac{1+s^2}{2})v(s-\delta,t) = \sin(\pi s(1-s)), \\ v_0(s) = 0, \Upsilon_1(0,t) = \Upsilon_2(1,t) = 0, T = 1. \end{cases}$$

Example 5.2.

Consider the following SPPPDDE:

$$\begin{cases} \left(\dfrac{\partial}{\partial t} - \varepsilon^2 \dfrac{\partial^2}{\partial s^2} + (2+s+s^2)\dfrac{\partial}{\partial s} \right) v(s,t) + (\dfrac{1+s^2}{2})v(s-\delta,t) = \sin(\pi s(1-s))t, \\ v_0(s) = 0, \Upsilon_1(0,t) = \Upsilon_2(1,t) = 0, T = 1. \end{cases}$$

6. Conclusion

We presented an $\varepsilon-$uniformly convergent numerical scheme to solve singularly perturbed parabolic partial differential-difference equation with a small negative shift in the spatial variable. In this scheme, the term with negative shift is approximated by using Taylor's series expansion. Then the resulting boundary value problem is approximated by employing the implicit Euler method for the temporal, and hybrid algorithm consisting of the midpoint method in the coarse mesh region and cubic spline method in the fine mesh region for the spatial discretization.

The computed $E_{\varepsilon,\delta}^{N,M}, r_{\varepsilon,\delta}^{N,M}, E^{N,M}$ and $r^{N,M}$ for the assumed examples with the various values of N and ε with $\delta = \eta = 0.5 \times \varepsilon$ are presented in Tables 1 though 4. From these tables, one can see that the $E_{\varepsilon,\delta}^{N,M}$ decreases as the step sizes decrease for all values of ε, and this ratifies an $\varepsilon-$uniform convergence of the proposed scheme.

As observed in Figures 1 (a) and (b), strong boundary layer is formed near $s = 1$ as $\varepsilon \to 0$. From Figures 2 (a) and (b), we observe that as the size of the delay parameter increases the thickness of the layer increases. The 3D view of the solution profiles plotted in Figures 3 (a) and (b) for Examples 5.1 and 5.2 respectively displace the boundary layer being on the right lateral domain. To depict the relationship between the $E_{\varepsilon,\delta}^{N,M}$ and the rate of convergence, we have used the log-log scale in Figures 4 (a) and (b) for Examples 5.1 and 5.2, respectively.

Acknowledgment:

The authors would like to thank the editor and referees for their constructive corrections to improve the quality of the paper.

REFERENCES

Adilaxmi, M., Bhargavi, D and Reddy, Y.N. (2019). An initial value technique using exponentially fitted non-standard finite difference method for singularly perturbed differential-difference equations, Appl. Appl. Math, Vol. 14, No. 1, pp. 245-269.

Andargie, A. and Reddy, Y.N. (2013). Solving singularly perturbed differential difference equations via fitted method, Appl. Appl. Math, Vol. 8, No. 1, pp. 318-332.

Bansal, K., Rai, P. and Sharma, K. K. (2017). Numerical treatment for the class of time dependent singularly perturbed parabolic problems with general shift arguments, Differential Equations and Dynamical Systems, Vol. 25, pp. 327-346.

Daba, I. T. and Duressa, G. F. (2020). Extended cubic b-spline collocation method for singularly perturbed parabolic differential-difference equation arising in computational neuroscience, International Journal for Numerical Methods in Biomedical Engineering, Vol. 37, No. 2.

Derstine, M., Gibbs, H., Hopf, F. and Kaplan, D. (1982). Bifurcation gap in a hybrid optically bistable system, Physical Review A, Vol. 26, pp.3720.

Doolan, E. P., Miller, J. J. and Schilders, W. H. (1980). *Uniform Numerical Methods for Problems with Initial and Boundary Layers*, Boole Press.

Glizer, V. (2000). Asymptotic solution of a boundary-value problem for linear singularly-perturbed functional differential equations arising in optimal control theory, Journal of Optimization Theory and Applications, Vol. 106, pp. 309-335.

Kumar, D. (2018). An implicit scheme for singularly perturbed parabolic problem with retarded terms arising in computational neuroscience, Numerical Methods for Partial Differential Equations, Vol. 34, pp. 1933-1952.

Kumar, D. and Kadalbajoo, M. K. (2011). A parameter-uniform numerical method for time-dependent singularly perturbed differential-difference equations, Applied Mathematical Modelling, Vol. 35, pp. 2805-2819.

Longtin, A. and Milton, J. G. (1988). Complex oscillations in the human pupil light reflex with mixed and delayed feedback, Mathematical Biosciences, Vol. 90, pp. 183-199.

Priyadharshini, R. M., Ramanujam, N., and Valanarasu, T. (2010). Hybrid difference schemes for singularly perturbed problem of mixed type with discontinuous source term, J. Appl. Math. Info, Vol. 28, pp. 1035-1054.

Ramesh, V. and Kadalbajoo, M. K. (2008). Upwind and midpoint upwind difference methods for time-dependent differential difference equations with layer behavior, Applied Mathematics and Computation, Vol. 202, pp. 453-471.

Ramesh, V. and Priyanga, B. (2019). Higher order uniformly convergent numerical algorithm for time-dependent singularly perturbed differential-difference equations, Differential Equations and Dynamical Systems, pp. 1-25.

Rao, R.N. and Chakravarthy, P.P. (2019). Fitted numerical methods for singularly perturbed one-dimensional parabolic partial differential equations with small shifts arising in the modelling of neuronal variability, Differential Equations and Dynamical Systems, Vol. 27, pp. 1-18.

Shishkin, G. I. (1988). A difference scheme for a singularly perturbed equation of parabolic type with discontinuous boundary conditions, USSR Computational Mathematics and Mathematical Physics, Vol. 28, pp. 32-41.

Stein, R. B. (1967). Some models of neuronal variability, Biophysical Journal, Vol. 7, pp. 37-68.

Tian, H. (2002). The exponential asymptotic stability of singularly perturbed delay differential equations with a bounded lag, Journal of Mathematical Analysis and Applications, Vol. 270, pp. 143-149.

Wazewska, M.-C. and Lasota, A. (1976). Mathematical models of the red cell system, Matematyta Stosowana, Vol. 6, pp. 976.

Woldaregay, M. M. and Duressa, G. F. (2019). Parameter uniform numerical method for singularly perturbed parabolic differential difference equations, Journal of the Nigerian Mathematical Society, Vol. 38, pp. 223-245.

Woldaregay, M. M. and Duressa, G. F. (2022a). Fitted numerical scheme for solving singularly perturbed parabolic delay partial differential equations, Tamkang Journal of Mathematics, Vol. 53.

Woldaregay, M. M. and Duressa, G. F. (2022b). Uniformly convergent numerical method for singularly perturbed delay parabolic differential equations arising in computational neuroscience, Kragujevac Journal of Mathematics, Vol. 46, pp. 65-84

Appendix

Table 1. $E_{\varepsilon,\delta}^{N,M}$ of Example 5.1 with $T = 1.0, \delta = 0.5 \times \varepsilon, M = N$

$\varepsilon \downarrow$	N=32	N=64	N=128	N=256	N=512
Proposed Method					
10^0	1.9998e-03	1.0844e-03	5.6678e-04	2.8994e-04	1.4670e-04
10^{-1}	5.5098e-03	3.3181e-03	1.9023e-03	1.0456e-03	5.5458e-04
10^{-2}	5.8712e-03	3.5891e-03	2.1232e-03	1.2098e-03	6.6900e-04
10^{-4}	5.8762e-03	3.5944e-03	2.1278e-03	1.2139e-03	6.7189e-04
10^{-6}	5.8762e-03	3.5944e-03	2.1278e-03	1.2139e-03	6.7189e-04
10^{-8}	5.8762e-03	3.5944e-03	2.1278e-03	1.2139e-03	6.7189e-04
Midpoint Upwind Method					
10^0	2.1994e-03	1.1778e-03	6.1092e-04	3.1142e-04	1.5725e-04
10^{-1}	7.4106e-03	4.6999e-03	2.8947e-03	1.7047e-03	9.6838e-04
10^{-2}	7.2526e-03	4.6756e-03	2.9359e-03	1.7694e-03	1.0286e-03
10^{-4}	7.2470e-03	4.6739e-03	2.9358e-03	1.7697e-03	1.0295e-03
10^{-6}	7.2470e-03	4.6739e-03	2.9358e-03	1.7696e-03	1.0295e-03
10^{-8}	7.2470e-03	4.6739e-03	2.9358e-03	1.7696e-03	1.0295e-03
Cubic Spline Method					
10^0	1.8277e-03	1.0130e-03	5.3456e-04	2.7472e-04	1.3931e-04
10^{-1}	8.8650e-03	4.6533e-03	2.3350e-03	1.1456e-03	5.6062e-04
10^{-2}	1.6202e-02	9.0831e-03	3.6470e-03	1.7450e-03	9.0803e-04
10^{-4}	1.6741e-02	1.0469e-02	5.8106e-03	3.0480e-03	1.5582e-03
10^{-6}	1.6741e-02	1.0469e-02	5.8109e-03	3.0486e-03	1.5582e-03
10^{-8}	1.6741e-02	1.0469e-02	5.8109e-03	3.0486e-03	1.5582e-03
Results in Kumar (2018)					
10^0	1.510e-03	7.590e-04	3.810e-04	1.910e–04	9.570e-05
10^{-1}	6.830e-03	4.030e-03	2.360e-03	1.350e-03	7.610e-04
10^{-2}	8.250e -03	4.910e -03	2.910e -03	1.680e -03	9.380e -04
10^{-4}	8.480e -03	5.130e -03	3.090e -03	1.810e -03	1.030e -03
10^{-6}	8.480e -03	5.130e -03	3.090e -03	1.810e -03	1.030e -03
10^{-8}	8.480e -03	5.130e -03	3.090e -03	1.810e -03	1.030e -03
Results in Daba and Duressa (2020)					
10^0	1.8395e-03	1.0160e-03	5.3522e-04	2.7487e-04	-
10^{-1}	7.3768e-03	4.4415e-03	2.3459e-03	1.1853e-03	-
10^{-2}	7.3987e-03	4.7136e-03	2.8435e-03	1.6478e-03	-
10^{-4}	7.3961e-03	4.7118e-03	2.8418e-03	1.6470e-03	-
10^{-6}	7.3961e-03	4.7118e-03	2.8417e-03	1.6470e-03	
10^{-8}	7.3961e-03	4.7118e-03	2.8417e-03	1.6470e-03	-

Table 2. $E^{N,M}$ and $r^{N,M}$ of Example 5.1 with $T = 1.0, \delta = 0.5 \times \varepsilon, M = N$

$\varepsilon \downarrow$	N=32	N=64	N=128	N=256	N=512
Proposed Method					
$E^{N,M}$	5.8762e-03	3.5944e-03	2.1278e-03	1.2139e-03	6.7189e-04
$r^{N,M}$	0.70913	0.75639	0.80971	0.85335	0.90419
Midpoint Upwind Method					
$E^{N,M}$	7.4106e-03	4.6999e-03	2.9359e-03	1.7697e-03	1.0295e-03
$r^{N,M}$	0.65696	0.67883	0.73030	0.7816	0.81624
Cubic spline Method					
$E^{N,M}$	1.6741e-02	1.0469e-02	5.8109e-03	3.0486e-03	1.5582e-03
$r^{N,M}$	0.67726	0.84929	0.93061	0.96827	0.98453
Results in Kumar (2018)					
$E^{N,M}$	8.48e-03	5.13e-03	3.09e-03	1.81e-03	1.03E-03
$r^{N,M}$	0.73	0.73	0.77	0.81	.84
Results in Daba and Duressa (2020)					
$E^{N,M}$	7.3987e-03	4.7136e-03	2.8435e-03	1.6478e-03	-
$r^{N,M}$	0.65	0.73	0.79	0.83	-

Table 3. $E_{\varepsilon,\delta}^{N,M}$ of Example 5.2 with $T = 1.0, \delta = 0.5 \times \varepsilon, N = M$

$\varepsilon \downarrow$	N=32	N=64	N=128	N=256	N=512
Proposed Method					
10^0	5.7811e-04	2.9885e-04	1.5194e-04	7.6609e-05	3.8466e-05
10^{-1}	1.3530e-03	7.8909e-04	4.2438e-04	2.1891e-04	1.1047e-04
10^{-2}	1.4572e-03	8.6051e-04	4.7185e-04	2.5755e-04	1.3466e-04
10^{-4}	1.4557e-03	8.5972e-04	4.7250e-04	2.5800e-04	1.3495e-04
10^{-6}	1.4556e-03	8.5970e-04	4.7249e-04	2.5799e-04	1.3494e-04
10^{-8}	1.4556e-03	8.5970e-04	4.7249e-04	2.5799e-04	1.3494e-04
Midpoint Upwind Method					
10^0	9.4867e-04	4.8465e-04	2.4500e-04	1.2318e-04	6.1761e-05
10^{-1}	3.7393e-03	2.3894e-03	1.4822e-03	8.9549e-04	5.2357e-04
10^{-2}	3.4630e-03	2.2148e-03	1.3799e-03	8.3307e-04	4.8796e-04
10^{-4}	3.4595e-03	2.2122e-03	1.3782e-03	8.3203e-04	4.8735e-04
10^{-6}	3.4595e-03	2.2122e-03	1.3782e-03	8.3202e-04	4.8734e-04
10^{-8}	3.4595e-03	2.2122e-03	1.3782e-03	8.3202e-04	4.8734e-04
Cubic Spline Method					
10^0	1.6943e-04	9.3315e-05	4.9098e-05	2.5207e-05	1.2774e-05
10^{-1}	1.6098e-03	7.4125e-04	3.1441e-04	1.6221e-04	8.2062e-05
10^{-2}	6.0150e-03	3.4445e-03	1.2304e-03	4.3554e-04	2.0100e-04
10^{-4}	6.2040e-03	3.9637e-03	2.2137e-03	1.1663e-03	5.9776e-04
10^{-6}	6.2039e-03	3.9637e-03	2.2137e-03	1.1665e-03	5.9831e-04
10^{-8}	6.2039e-03	3.9637e-03	2.2137e-03	1.1665e-03	5.9831e-04

Table 4. $E^{N,M}$ and $r^{N,M}$ of Example 5.2 with $T = 1.0, \delta = 0.5 \times \varepsilon, N = M$

$\varepsilon \downarrow$	N=32	N=64	N=128	N=256	N=512
Proposed Method					
$E^{N,M}$	1.4572e-03	8.6051e-04	4.7258e-04	2.5804e-04	1.3496e-04
$r^{N,M}$	0.7599	0.8646	0.8730	0.9351	0.95380
Midpoint Upwind Method					
$E^{N,M}$	3.7393e-03	2.3894e-03	1.4822e-03	8.9549e-04	5.2357e-04
$r^{N,M}$	0.64612	0.68891	0.72699	0.77429	0.83724
Cubic Spline Method					
$E^{N,M}$	6.2040e-03	3.9637e-03	2.2137e-03	1.1665e-03	5.9831e-04
$r^{N,M}$	0.6464	0.8404	0.9243	0.9632	0.98295

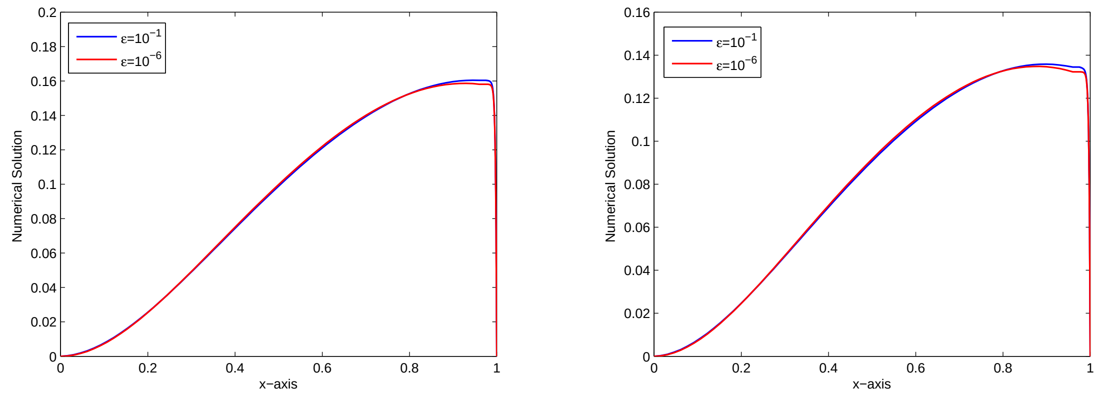

(a) (b)

Figure 1. Effect of ε on the solution behavior at $T = 1, \delta = 0.5 \times \varepsilon, N = M = 128$ for (a) Example 5.1 and (b) Example 5.2

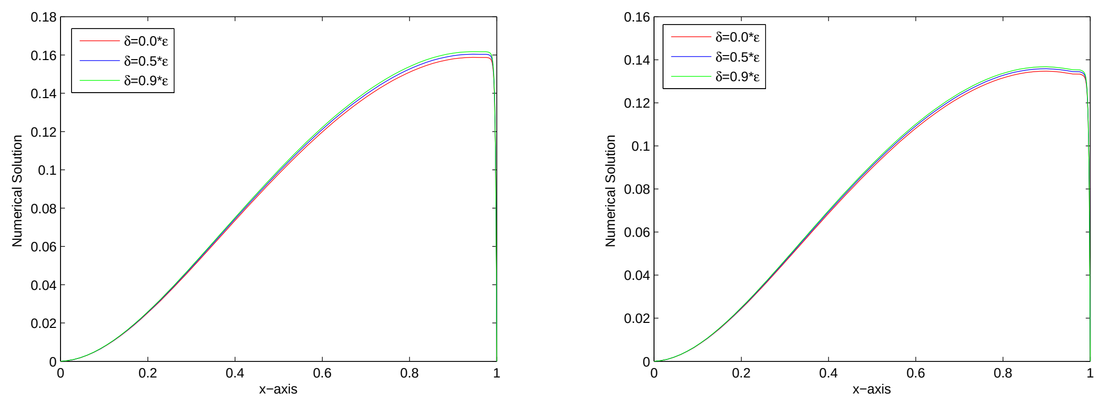

(a) (b)

Figure 2. Effect of δ on the solution behavior at $T = 1, \varepsilon = 10^{-1}, \eta = 0.5 \times \varepsilon, N = M = 128$ for (a) Example 5.1 and (b) Example 5.2

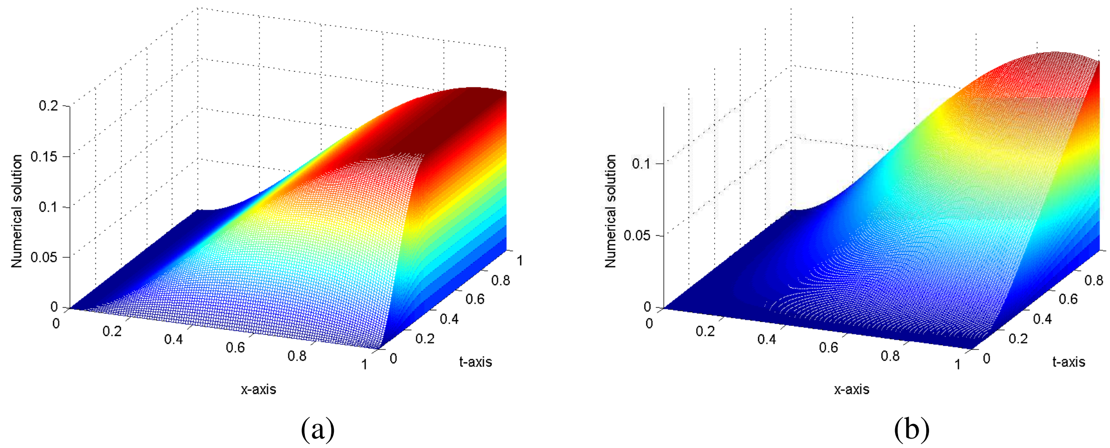

Figure 3. Numerical solution profiles at $T = 1.0, \delta = 0.5 \times \varepsilon, \eta = 0.5 \times \varepsilon, \varepsilon = 10^{-6}, N = M = 256$ for (a) Example 5.1 and (b) Example 5.2

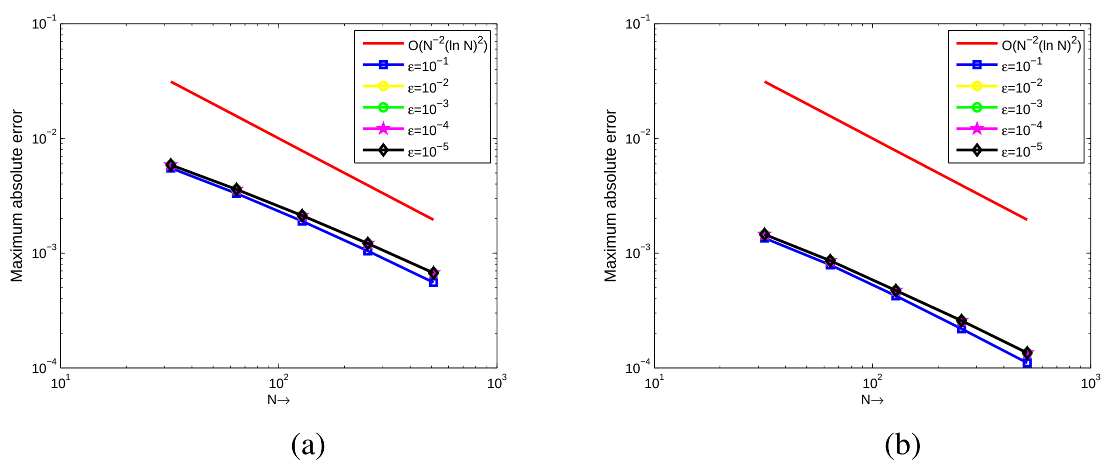

Figure 4. Log-Log scale for (a) Example 5.1 and (b) Example 5.2